



# The Economic Dynamics After a Flood: Evidence from Satellite Data

Dino Collalti<sup>1</sup>

Accepted: 22 May 2024  
© The Author(s) 2024

## Abstract

This study investigates the effect of flash floods on local economic activity in Central America and the Caribbean. I measure these rarely analyzed floods by constructing a high-resolution, physically based index of flash flood occurrence from satellite data and connect these to changes in local night light emissions. After accounting for tropical cyclone activity, flash floods have a delayed, short-term negative effect on economic activity. In countries with a low to medium human development index (HDI), the average negative effect can be up to 5.6% in the following months. Countries with higher HDI appear more resilient and are only marginally affected. Also, flash floods exhibit a minor positive spatial spillover in low to medium HDI countries, besides their more substantial local negative effect. Due to their high frequency, flash floods have a detrimental effect on local economic growth in developing countries that will likely be exacerbated by climate change. (JEL )

**JEL Classification** O11 · Q54 · R11

## 1 Introduction

When Tropical Storm Ophelia poured extreme rainfall over New York City on September 29th in 2023, the resulting flash floods wreaked havoc: the city shut down its subway, roads, and airport terminals, and a state of emergency had to be declared. Less than a week before, heavy rainfall in the night caused a flash flood early on the 25th near Guatemala City when a small river broke its banks, destroying several homes and causing deaths and missing people.<sup>1</sup> These are not isolated incidents. According to the Emergency Events Database (EM-DAT), 0.9 Million people were affected by flash floods in 2022, the 5th most among all natural hazard subtypes.<sup>2</sup> In addition, the frequency and severity of flash floods are projected to increase with climate change (IPCC 2023). The Caribbean and

<sup>1</sup> See the FloodList program news funded through the European Union's Copernicus scheme.

<sup>2</sup> After droughts (107 Million), tropical cyclones (15 Million), earthquakes (3.6 Million), and convective storms (1.6 Million) but before river floods (0.1 Million) and forest fires (0.03 Million).

---

✉ Dino Collalti  
dino.collalti@windowslive.com

<sup>1</sup> Department of Economics, Center for Regional Economic Development, University of Bern, Schanzeneckstrasse 1, 3012 Bern, Switzerland

Central America are especially at risk from flash floods by being already one of the world's most rainfall- and thunderstorm-heavy regions. Further aggravating the risk, urbanization is often unregulated, and soil degradation is common (Pinos and Quesada-Román 2021). Therefore, understanding how flash floods impact economic activity in Central America and the Caribbean is crucial for its development. This study contributes to this understanding by physically modeling flash flood events from satellite rainfall data and connecting these to changes in night light activity while controlling for tropical cyclone activity and local characteristics.

While the direct physical damage from natural hazards is self-evident, the overall economic consequences are not. In many countries, natural disasters are a major channel through which climate and environmental degradation impact the economy and lower development (Felbermayr and Gröschl 2014). A growing literature has thus started to study the economic impacts of various types of natural disasters: tropical storms (Strobl 2012; Hsiang 2014; Deryugina 2017; Ishizawa and Miranda 2019; Kunze 2021), earthquakes (Barone and Mocetti 2014; Fabian et al. 2019), droughts (Barrios et al. 2010; Hornbeck 2012) and urban floods (Kocornik-Mina et al. 2020), to name a few. Many estimate the overall economic impact of the natural disaster, while others are explicitly entertaining the notion of direct (first-order) and indirect (second-order) effects. The direct impact can be viewed as the immediate destruction and rebuilding cost. The indirect impact is characterized by second-order effects such as the re-organization of the economy. For instance, when an establishment is destroyed, this disrupts the value chain. Similarly, if a firm goes out of the market, the now laid-off workers will be subject to unemployment. These second-order effects are often considerable. Deryugina (2017) finds that US hurricanes substantially increase transfers such as unemployment benefits to affected counties, significantly exceeding direct disaster assistance in value.

The literature quantifying the impact of extreme rainfall and flood events specifically can be divided into two groups. Those concerned with extreme rainfall use aggregated weather data such as the region-specific deviation in monthly rainfall to estimate economic impacts of weather anomalies (Dell 2012, 2014; Felbermayr et al. 2022; Kotz et al. 2022). These studies implicitly evade many flash flood events because a monthly measure of rainfall cannot reliably identify short (usually less than a day) extreme rainfall events. The other group uses flood report data instead to overcome this issue (Loayza et al. 2012; FombyFomby et al. 2013; Kocornik-Mina et al. 2020). The advantage of flood report data like EM-DAT or the Dartmouth Flood Observatory (DFO) is that it identifies the natural hazard by impact. But it also comes at a cost: relying on media reports like the EM-DAT to identify and locate flood events introduces reporting, selection, and endogeneity biases (Panwar and Sen 2020). For example, insurance penetration and reported damages are highly correlated with a country's development (Felbermayr et al. 2022). The DFO instead relies on satellite imagery on cloud-free days to quantify the flooded area. Since flash floods have a short lifespan and occur in combination with heavy rainfall and thus cloud coverage, many go unnoticed. To the best of my knowledge, no study focuses on the economic impact of flash floods, as there is no consistent nor exhaustive database of them. It is thus necessary to develop a physically consistent index of occurrence that reliably identifies flash flood events to study their economic impacts.

Macroeconomic models of natural disasters are generally based on classical growth theory with the event as a one-time shock to the capital stock (Hallegatte et al. 2007; Strulik and Trimborn 2019). However, it has been argued that these models cannot capture the effects of short-term shocks from natural hazards adequately to derive long-term impacts (Cavallo et al. 2013). Regardless of this debate, the economic impact has to be

assessed empirically to provide estimates for model parameters (Strulik and Trimborn 2019). This impact has to be estimated for each hazard separately since they are not necessarily comparable. Some might destroy a larger share of certain types of capital, some damage a larger share of public infrastructure, and others displace more people. It has also been recognized that with climate change making natural hazards more common in many parts of the world, jointly considering events based on their frequency and intensity is crucial when estimating the effects on growth. For instance, in a Solow-like model that allows for non-equilibrium dynamics, Hallegatte et al. (2007) show a sharp increase in GDP losses if natural hazards intensity or frequency increase above a certain threshold. The capacity of an economy to cope with a natural hazard, determining the threshold, is linked to its development (Hallegatte and Dumas 2009). For instance, the more developed economy can cope better with severe and frequent shocks to its infrastructure as it has the necessary means for timely reconstruction.

To frame the analysis, there are four hypotheses about an economy's growth dynamics after a natural disaster: a return to the same output level after an initial decline, a decline in output level without recovery, or an increase in the level of output either immediately with creative-destruction or after some time as build-back-better (Botzen et al. 2019). The question of which hypothesis is most adequate, focusing on high-impact natural disasters, has not reached a conclusive answer (Skidmore and Toya 2002; Cuaresma 2008; Klomp 2016). Most evidence points towards an initial decline in output that gradually recovers over time. In contrast, the no-recovery, build-back-better, and creative-destruction hypotheses have support in specific settings (Strobl 2012; Felbermayr and Gröschl 2014; Noy and Strobl 2023). It is suggested that this depends mainly on the type of disaster, the time period and geographic scope of the analysis (Lazzaroni and van Bergeijk 2014; Klomp and Valckx 2014). Critically, the scale of analysis matters. Economic mechanisms that would cause output to increase are typically motivated on the micro- or perhaps city level. For example, local build-back-better might siphon investments into an area affected by a natural disaster at the cost of other locations. Similarly, the negative impact might be relatively short-term such that rebuilding is completed within a year. It follows that country-by-year panel data is not well suited considering the growth dynamics of a small-scale, high-frequency natural hazard such as flash floods. However, if one is interested in the aggregate net effect, that is the effect of the natural hazard after spatial equilibrium effects and temporal smoothing took place, then estimates from a country by year panel are informative.

Therefore, a critical part of the methodology is to detect extreme rainfall events that likely trigger flash floods on a high spatial and temporal resolution. I use the flash flood intensity-duration classification from Collalti et al. (2024) as a physical measure for flood incidence. This classification is based on intensity-duration-frequency (IDF) curves from conditional copula sampling and exhaustive information on all flash flood events in Jamaica from 2001 to 2018. Jamaica shares a similar topography, soil composition, and climate with the whole region of Central America and the Caribbean, so the classification is well-calibrated. I use rainfall information from the Integrated Multi-satellitE Retrievals for GPM (IMERG), which employs the Global Precipitation Measurement (GPM) constellation satellite data. This allows the construction of meteorologically distinct rainfall events by imposing some inter-event-time without any rainfall from the high frequency (half-hourly) satellite data for each  $0.1^\circ \times 0.1^\circ$  (approx. 11 km  $\times$  11 km at the equator) cell. Events can, therefore, stretch over several days, whereby most events last less than a day. Of the 64 M cell-wise rainfall events in Central America and the Caribbean in 2000–2021, 2.3 M or approximately 1.7% can be classified as flash floods.

I estimate a flash flood's effect on aggregate economic activity by using satellite images of night lights at a monthly frequency. The source of night light data is NASA's Black Marble product that removes cloud-contaminated pixels and corrects for atmospheric, terrain, vegetation, snow, lunar, and stray light effects on the VIIRS Day/Night Band (DNB) radiances. Controlling for tropical storms and various fixed effects, I find that night lights decrease significantly by up to 5.6% in the following months for low and medium-development countries. Afterward, there is a quick recovery within the first year. Due to their high frequency, night light growth decreases significantly due to flash floods for locations in the region's low- and medium-developed countries. The reaction in night lights is considerably less pronounced in high- and very high-development countries.

These results are important for several reasons. First, the findings contribute to the literature on physically modeled natural disasters in economics (Nordhaus 2010; Hsiang 2014; Eichenauer 2020). Second, extreme rainfall events and the associated pluvial floods are, after droughts, the extreme events most likely to increase in probability and intensity due to climate change (Seneviratne et al. 2021). For instance, the 6th IPCC Report states that "*Projected increases in direct flood damages are higher by 1.4 to 2 times at 2°C and 2.5 to 3.9 times at 3°C compared to 1.5°C global warming without adaptation.*" (IPCC 2023). Knowledge of how a natural hazard shock affects the economy is necessary to adequately inform policymakers about climate change risks.

The remainder of the paper is organized as follows: Sect. 2 presents the study region, describes the data, discusses difficulties in measuring flash floods, and provides summary statistics. Section 3 focuses on the role of geography in flash flood risk. In Sect. 4, the identification strategy is detailed, whereas Sect. 5 provides results which are discussed in Sect. 6. Finally, Sect. 7 concludes.

## 2 Data

Three types of data are necessary for this study. First, data on hazards includes a satellite-derived rainfall measure and the subsequent creation of a flash flood indicator as the variable of interest. In addition, I construct an index of hurricane destructiveness. Second, comes the economic data, where I use night light data to infer changes in economic activity. Third, auxiliary data on topography and land use serve as sources for potential heterogeneity.

### 2.1 Study Region

The study region of Central America and the Caribbean is characterized by its proximity to the sea: no location is further away from it than 200 km (Encyclopedia Britannica 2022). The tropical climate is tempered by elevation, latitude, and local topography. Rainfall occurs in a dry and wet season pattern and is heaviest between May and November. Topography is diverse: most countries have humid lowlands along the coast, while there are pronounced hills and mountain ranges. Natural vegetation is equally varied. Tropical forests occupy lowlands, while evergreen forests clothe hills and mountains. However, much of Central America and the Caribbean's timberland has been cleared for crop cultivation.

## 2.2 Flash Floods

Floods come in various forms that determine the flood hazard and risk. Floods caused by local excess rainfall, so-called pluvial floods, can be divided into surface water floods and flash floods. Surface water floods are caused when rain falls over a prolonged period such that the drainage systems and general runoff cannot deal with the amount of water, resulting in a shallow, standing flood. Flash floods, on the other side, are characterized by shorter, more intense extreme rainfall events. Torrential rainfalls trigger these dangerous floods due to their quick onset and ravageous, debris-sweeping flow. They are a predominantly localized phenomenon that can occur almost everywhere and is difficult to forecast.

### 2.2.1 From Rainfall to Floods

In this study, flash floods are measured via a binary classification that indicates whether, in a month, an episode of heavy rainfall likely triggered some flash flood at a location. This classification borrows from Collalti et al. (2024), who employ a hydro-statistical methodology and exhaustive data on confirmed flash flood events in Jamaica to estimate a decision rule for the optimal classification of flood incidence. Specifically, the procedure starts by first defining appropriate rainfall events that relate to actual weather conditions via an inter-event time definition, where 12 h without rainfall above 0.1 mm/h meteorologically delimits a rainfall event from another. This allows for a varying duration of rainfall events while not suffering from arbitrary cut-offs as, for instance, daily rainfall measures would. Figure 1 depicts this procedure that takes as input rainfall time series and yields meteorologically distinct rainfall events. By using remote sensing data from the Global Precipitation Measurement (GPM) Integrated Multi-satellitE Retrievals (IMERG) on a  $0.1^\circ \times 0.1^\circ$  (approx. 11 km  $\times$  11 km at the equator) grid with half-hourly data, coverage is consistent for the whole study region (Huffman et al. 2015). I run the IETD event definition on all 13,702 GPM/IMERG cells in the study region, where each cell's rainfall time series has a length of approximately 368,000.

Most of the resulting events are non-hazardous regular rainfall events that are not hazardous. However, the more extreme an event becomes, the more likely it triggers a local flash flood. In hydrological research that aims to quantify pluvial flood risk, this extremeness is characterized by the average intensity (mm/h) and duration (h) of events in so-called intensity-duration-frequency (IDF) curves (Koutsoyiannis et al. 1998). For a set duration or intensity, a rainfall event becomes less frequent (and more extreme) if either duration or intensity increases, which are themselves negatively correlated (Endreny and Imbeah 2009). The IDF curve, therefore, shows all combinations of intensity and duration for a given return period where a higher return period corresponds to more extreme events.

Collalti et al. (2024) use the local yearly maximum rainfall events in terms of total rainfall to generate IDF curves for extreme rainfall events in Jamaica via copula functions. That way, the non-linear dependence between intensity, duration, and frequency is flexibly characterized. Equipped with all the confirmed, time- and geo-referenced flash floods in Jamaica from 2001 to 2018, they evaluate which IDF curve best predicts the occurrence of a flash flood for all extreme rainfall events and achieve a true positive rate of 65% for events above the IDF curve with a return period of  $2\frac{1}{6}$  years.

### 2.2.2 Flash Flood Indicator

I employ this IDF curve as a binary flash flood decision rule on the same satellite-based rainfall estimate to recover potential flood events. The GPM/IMERG satellite precipitation algorithm combines various microwave and infrared precipitation measurements to produce precipitation estimates adjusted with surface gauge data. The sample period is June 1st 2000 to June 30th 2021. For every month with one rainfall event above the threshold, the corresponding GPM/IMERG grid cell area is considered treated by a flash flood.<sup>3</sup>

Since the IDF curve was developed to maximize the ratio of true positives against false positives, it gives equal weights to both. Here, false positives are a more significant concern than missing some true positives. For instance, false positives lead to non-classical measurement error in our variable of interest and subsequently bias the results. On the other side, missing some true positives only reduces the number of detected events and precision while not causing bias.

In addition, rainfall events for the  $2\frac{1}{6}$  return period that maximized the ratio of true positives against false positives in Jamaica is, on average, 3.7 mm/h lower than rainfall events with the same return period for the whole study region in this paper. While this does not imply that the indicator should be adjusted for that amount, it indicates that some adjustments are necessary to avoid many false positives in particularly rainfall-heavy regions. As a starting point for subsequent analysis, I require that a rainfall event has an intensity of at least 2 mm/h above the IDF curve to be classified as a flash flood. If an event exceeds this threshold, I treat it as a flood-causing rainfall event.

In the study region, one of the most rainfall-intense regions in the world, locations defined by the GPM/IMERG grid experience a flash flood 1.7 times each year on average, according to the index. There is considerable spatial variation for the average occurrence probability and spatial clustering for a given month, as Fig. 2 shows. Table 1 provides summary statistics of all rainfall events. Flash flood rainfall events are, on average, 5.5× more intense and 2.5× longer than non-flash flood events.

### 2.3 Night Lights

The source of night light data is NASA's Black Marble product. Black Marble processing of the Visible Infrared Imaging Radiometer Suite (VIIRS) Day-Night Band (DNB) removes cloud-contaminated pixels and corrects for atmospheric and other light effects such as gas flares, is calibrated across time, and validated against ground measurements (Román et al. 2018). The VIIRS DNB provides global daily measurements of nocturnal visible and near-infrared light. The VIIRS DNB is said to be ultra-sensitive in low light conditions, making it suitable for monitoring remote areas as well as highly urbanized locations.

Night lights have been used increasingly as a proxy of local economic activity in developing countries (Hodler and Raschky 2014; Storeygard 2016; Kocornik-Mina et al. 2020). In their seminal paper, Henderson (2012) lay foundations on using night light data to augment income growth measures. They find that the elasticity between the growth of lights and local GDP growth is around 0.3. Chen and Nordhaus (2019) compare DMSP/OLS and VIIRS for predicting the US's cross-sectional and time-series GDP data. They find that VIIRS performs well at predicting metropolitan area night light growth. Gibson et al.

<sup>3</sup> Flash floods that start in one month and end in the next are only assigned to the month when the rainfall event started.

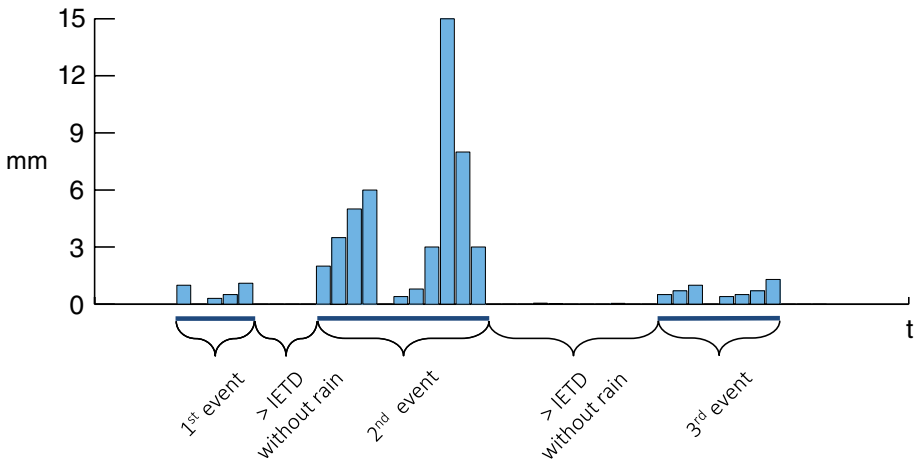


**Fig. 1** Rainfall event definition. *Notes:* Illustration of the event definition via inter-event-time (IETD). In the GPM/IMERG data, each step in time corresponds to a half-hourly interval with a rainfall measurement per grid cell. Each grid cell has a time series of approximately 368,000 half-hourly observations. Each of these 13,702 time series is then split into distinct events via a 12 h IETD. This means that if there is at least 12 h without rainfall to the next episode of rainfall, these two constitute single events (1st and 2nd event). If there is less than 12 h without rainfall in between, it is treated as a single event (2nd event). This process is applied to the whole time series (3rd event, etc.) and repeated for all cells. Each event is then assigned its start time and cell coordinates

(2021) compare the ability of the DMSP/OLS and VIIRS to predict local GDP for Indonesia and finds that the DMSP/OLS is twice as noisy as the VIIRS.

I use version VNP46A3, which provides monthly composites generated from daily observations. Monthly composites remove much of the noise in daily observations and also ensure continuous measurements even when there is cloud coverage for several days in a row, which is not uncommon in the tropics. Black Marble has been available globally since January 2012 on a 15 arc-second (approx. 500 m) linear latitude-by-longitude grid. Figure 3 shows lights at night in January 2012. All cells not on land are removed for the analysis—including both ocean and lakes. The Black Marble data is aggregated to the lower-resolution GPM/IMERG grid cells such that each night light observation in the empirical analysis is the sum of the 576 Black Marble observations.

## 2.4 Tropical Storms

In analyzing the effect of floods, which are due to extreme rainfall in the Caribbean and Central America, it is necessary to separate the flood effect from the effect of tropical storms' wind destruction. I follow Strobl (2011) in calculating the local wind exposure during a storm with the Boose et al. (2004) version of the Holland (1980) wind field model. The source of storm data used is the HURDAT Best Track Data (Landsea and Franklin 2013). “Appendix” provides additional information on the wind field model. The resulting wind speed  $V_{ijt}$  is then translated to a hurricane destruction index  $wn_{it}$  of economic impact via the non-linear damage function by Emanuel (2011), see for instance Brei et al. (2019):

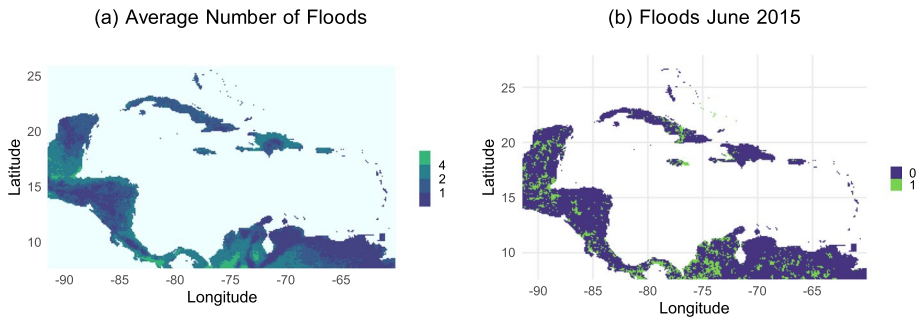


**Fig. 2** Map of flash flood distribution. *Notes:* Map of the spatial distribution of flash floods according to the indicator in Sect. 2.2.2. The primary GPM/IMERG rainfall data is first aggregated to a series of distinct events per grid cell via the inter-event-time definition in Sect. 2.2.1. Then, if an event exceeds the IDF threshold from Collalti et al. (2024) by more than 2 mm/h in average intensity, it is classified as a flash flood. **a** Then plots the average number of such flash floods per year from June 2000 to October 2021 and **b** maps the flash flood incidents in June 2015

**Table 1** Rainfall and flash flood summary statistics

Statistic	Mean	St. dev.	Min	Median	Max
<i>Flash Flood Rainfall Events (N = 1,056,508)</i>					
Intensity mm/h	6.61	3.31	3.93	5.50	113.18
Duration h	16.60	11.14	1.00	13.50	214.50
Year	2009.44	5.79	2000	2009	2021
Month	7.02	2.99	1	7	12
Longitude	-80.15	8.28	-91.95	-81.55	-58.05
Latitude	16.07	8.07	7.05	14.25	31.95
<i>Non Flash Flood Rainfall Events (N = 63,049,303)</i>					
Intensity mm/h	1.21	1.36	0.10	0.77	190.22
Duration h	6.65	10.84	0.50	3.50	3875.00
Year	2010.49	6.12	2000	2011	2021
Month	6.83	3.05	1	7	12
Longitude	-78.00	9.22	-91.95	-79.65	-58.05
Latitude	15.73	7.54	7.05	13.95	31.95

Summary statistics of all flash flood and rainfall events characteristics. Intensity refers to the average hourly intensity of an event

$$wn_{it} = \frac{v_{ijt}^3}{1 + v_{ijt}^3} \times 100 \quad (1)$$

with

$$v_{ijt} = \frac{\max(V_{ijt} - V_{thresh}, 0)}{V_{half} - V_{thresh}} \quad (2)$$



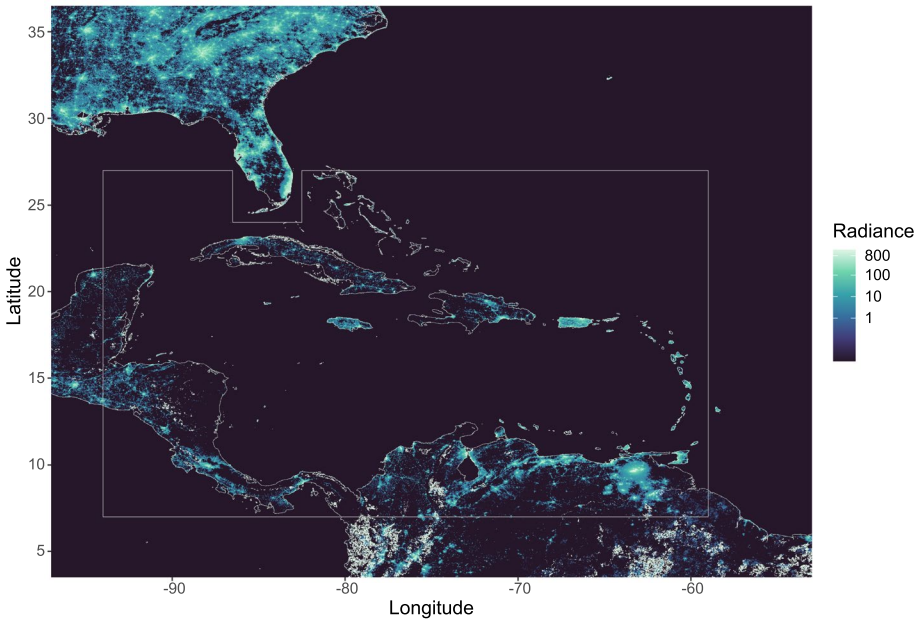


**Fig. 3** Map of night lights. *Notes:* Night light map in January 2012 from NASA's VNP46A3 Black Marble product of the Visible Infrared Imaging Radiometer Suite (VIIRS) Day-Night Band (DNB) that removes cloud-contaminated pixels and corrects for atmospheric and other light effects such as gas flares, is calibrated across time, and validated against ground measurements. The grey polygon indicates the study region of Central America and the Caribbean, excluding Florida. The radiance in the figure is top-coded at  $800 \text{ W}/(\text{cm}^2 - \text{sr})$  to shrink the color scale and make differences at lowly lit places visible. Due to ships, some cells do have night light activity, even if not on land. For the analysis, all cells not on land are removed

where  $V_{ijt}$  corresponds to the maximum wind speed of hurricane  $j$  in location  $i$  at time  $t$ . Then,  $V_{thresh} = 92 \text{ km/h}$  is the lower threshold below which no damages occur, whereas  $V_{half} = 203 \text{ km/h}$  is where 50% destruction is expected. Conveniently, a one-unit increase can be interpreted as a 1% increase in damages. The maximum  $v_{ijt}$  in a given month represents the tropical cyclone impact in subsequent analysis.

## 2.5 Summary Statistics

Table 2 displays summary statistics. There are 13,702 cells with 114 monthly observations starting in January 2012 and ending in June 2021 for a panel of 1.56 Million observations.<sup>4</sup> Out of these 1.56 Million observations, 150,065 or 9.6% are potentially hit by a flash flood. Observations that are hit emit less light at night on average ( $3.72$  vs.  $6.52 \text{ W}/(\text{cm}^2 - \text{sr})$ ), have, on average, been hit more frequently per year in the period 2000–2010 (8.0 vs. 6.7 times), have a lower average elevation (242.7 m vs. 331.3 m) and have a slightly less rugged terrain (14.39 vs. 16.12 TRI).<sup>5</sup> In summary, the two groups of observations are not

<sup>4</sup> The rainfall data has been available since 2000. Thus, lags of flood events before 2012 have been supplemented to the panel.

<sup>5</sup> Data on land use and topography is described in Section “Land Cover” and “Topography” in the “Appendix”.

equal; local characteristics and seasonality likely affect whether a flash flood occurs. The subsequent empirical analysis has to consider these differences.

### 3 The Role of Geography in Flash Flood Risk

The flash flood indicator derived in Sect. 2.2 only considers the intensity and duration of rainfall, omitting geography. Naturally, one might wonder whether the accuracy could be improved by considering features like land use, elevation, or terrain ruggedness from Section “Land Cover” and “Topography”. For instance, Wheater and Evans (2009) highlight the role of soil permeability for flood risk, which is negatively influenced by urbanization, deforestation and intensification of agricultural practice. Similarly, Hounkpè et al. (2019) document that land use change from natural vegetation towards farmland increases flood risk. These studies, however, focus on floods in highly localized catchment areas, where counterfactuals in risk are difficult to come by.<sup>6</sup> The objective of such studies is the precise water flow modeling and not the counterfactual question of how flood risk changes by land use in general. It stands to be established how land use and topography aggregated to locations corresponding to gridded remote sensing rainfall observations can inform flash flood risk.

Suppose aggregate land use or topography can be used to improve the flash flood indicator. In that case, land use or topography should have a statistically significant effect on the probability of observing a confirmed flood event after controlling for the indicator. Borrowing the data on the confirmed flash flood events in Jamaica from 2001 to 2018 and the yearly maximum rainfall events at all locations affected from Collalti et al. (2024), regressing the confirmed flash flood on the flash flood indicator, land use shares, and topography determines whether land use or topography has a direct influence. Alternatively, one could also suspect that each aspect of geography does not directly influence the flash flood risk but instead works through extreme rainfall and the indicator, which can be examined in an interaction term. Table 3 reports the corresponding logistic regression results.

Comparing the estimate for the flash flood indicator across specifications in Table 3, the indicator predicts the observed occurrence of a flash flood well. The odds of observing a flash flood increase by 84–97% in the case of the flash flood indicator equal to one and is statistically significant across specifications. Note that the sample consists only of yearly maximum rainfall events and the actual confirmed flash flood rainfall events—a regression of all rainfall events would yield vastly stronger effects but would hardly be reasonable. Neither elevation, terrain ruggedness (TRI), nor share of built area, cropland, grassland, and forest cover significantly change the odds of observing a flash flood after controlling for the flash flood indicator. The direct effect of the indicator is also robust against an interaction with the dominant land use type in column (3).<sup>7</sup>

It might be that the rainfall flash flood indicator already implicitly takes some of the flash flood risk due to geography into account. For instance, we expect a higher flash flood risk for higher altitudes and rugged terrain (“Mountains”), where we also observe more extreme rainfall events. Similarly, there is generally more natural vegetation in the most rainfall-heavy areas in the case of Jamaica. Refining the flash flood indicator by incorporating local geography does not present itself as necessary, as it is questionable whether

<sup>6</sup> Another example is Abdelkareem (2017) who maps flash flood risk for a specific catchment (“Wadi”) in Egypt, using remote sensing data on rainfall, elevation, soil, and others.

<sup>7</sup> Built<sub>majority</sub> and Agriculture<sub>majority</sub> refer to cells which have a share of built area above the 2/3 quantile or a share of cropland plus grassland above the 2/3 quantile, respectively.

**Table 2** Summary statistics

Statistic	Mean	St. dev.	Min	Median	Max
<i>Flash flood cell × month observations (N = 150,065)</i>					
Night light	3.72	27.03	0.001	0.65	4442.77
Wind index	0.02	1.27	0.00	0.00	319.76
# Historical floods	8.00	1.85	1	9	10
Longitude	- 78.75	8.17	- 91.95	- 77.35	- 60.05
Latitude	12.11	4.69	7.05	9.65	26.75
Year	2015.82	2.77	2012	2016	2021
Month	7.62	2.55	1	8	12
Elevation m	242.68	337.65	-0.52	113.31	3486.03
Terrain ruggedness	14.39	16.10	0.00	6.77	96.39
Forest area %	44.87	26.81	0.00	38.84	99.99
Built area %	0.94	3.38	0.00	0.17	84.22
<i>Non flash flood cell × month observations (N = 1,403,071)</i>					
Statistic	Mean	St. dev.	Min	Median	Max
Night light	6.52	63.19	0.001	0.53	7010.11
Wind index	0.01	0.79	0.00	0.00	327.47
# Historical floods	6.71	2.17	1	7	10
Longitude	- 77.20	9.43	- 91.95	- 76.25	- 60.05
Latitude	13.06	4.81	7.05	11.25	26.75
Year	2016.31	2.74	2012	2016	2021
Month	6.20	3.50	1	6	12
Elevation m	331.30	480.71	- 0.52	131.38	3612.71
Terrain ruggedness	16.12	18.54	0.00	6.82	104.42
Forest area %	44.09	26.00	0.00	39.50	99.99
Built srea %	1.19	3.97	0.00	0.20	84.22

Summary statistics of the final panel data. The top panel summarizes data for the observations with a flash flood, whereas the bottom panel does so for the other observations

it might improve predictive performance. Instead, I explore heterogeneity in economic impact due to geography in Sect. 5.4.

## 4 Empirical Strategy

To develop an empirical strategy, we first need to consider the nature of the phenomenon studied, our variable of interest, and its relation with the outcome. The variable of interest is a binary indicator of whether, within a given month and a specific location, a rainfall episode was so extreme that there was likely a flash flood in the area. For identification, a Difference-in-Differences (DiD) setup with fixed effects is suggested—the panel structure of the data readily allows for the estimation of such a model with ordinary least squares (OLS). Three assumptions must be fulfilled for a causal interpretation of the effects: no anticipation effect, parallel trends, and linear additive effects. In the case of extreme weather events, these can be satisfied. Weather, especially extreme rainfall, is nigh impossible to forecast for horizons longer than two weeks. There is seasonality in the likelihood

**Table 3** Logit regressions: SFF-indicator and geography

Dependent variable Model	Confirmed flash floods		
	(1)	(2)	(3)
(Intercept)	- 2.5*** (0.14)	0.59 (4.2)	0.87 (4.3)
FF-indicator	0.61** (0.29)	0.63** (0.30)	0.68* (0.41)
Elevation m		- 0.0004 (0.001)	- 0.0002 (0.001)
TRI		- 0.01 (0.02)	- 0.02 (0.02)
% Built area		- 0.02 (0.05)	- 0.006 (0.05)
% Cropland		- 0.04 (0.09)	- 0.04 (0.09)
% Grassland		- 0.07 (0.06)	- 0.08 (0.06)
% Forest cover		- 0.02 (0.05)	- 0.02 (0.05)
FF-indicator $\times$ built <sub>majority</sub>			- 1.0 (0.86)
FF-indicator $\times$ agriculture <sub>majority</sub>			0.82 (0.69)
Observations	935	935	935
Pseudo R <sup>2</sup>	0.00760	0.02005	0.02844

*Standard-errors in parentheses. Signif. Codes: \*\*\*: 0.01, \*\*: 0.05, \*: 0.1*

Results from a logistic regression of the binary indicator of confirmed flash floods on the flash flood indicator derived in Sect. 2.2.2, elevation, a terrain ruggedness index (TRI) and % share of land use by area

of an extreme event, with seasons that are heavy in rain and seasons that are dry. Further, not all places bear the same risk: some areas close to mountains or in the path of persistent, high-moisture wind systems are more likely than others to experience extreme rainfall. Even then, knowing the underlying probability of extreme events in a location or during a specific time of the year does not allow us to predict the occurrence of a single event with sufficient confidence in weather forecasts. Reversing that argument means that, given location and season, no further observable characteristics would lead to selection bias. Thus, there is a quasi-randomness in the occurrence of a flood that can be exploited to estimate a causal effect when controlling for observed differences in flash flood risk.

Some extreme rainfall episodes are likely attributable to tropical cyclones (TCs). Including the wind index derived in Sect. 2.4 separates the effect of TC wind damage from extreme rainfall. Similarly, there might be a spatial spillover of flood events across cells, including an index of floods in neighboring cells' controls for potential spatial spillovers.<sup>8</sup> Assessing the dynamic response heterogeneity concerning geography or a country's development while controlling for the dynamics due to tropical storms and spillovers demands a model with clear serial correlation of the lagged indicators. Constructing impulse response functions (IRFs) would entail extrapolating from coefficient estimates at increasingly distant horizons. Instead, I use local projections introduced by Jordà (2005) and recently employed in the context of natural hazards by Naguib et al. (2022) to study dynamic changes in night light due to tropical storms in India. Local projections are performed as a set of sequential regressions, where the dependent variable is shifted  $m$  steps ahead instead of introducing  $m$  lags of the flood indicator. An additional benefit of the local projection method is that it directly yields impulse-response functions with correctly specified confidence bands. The specification I use is

<sup>8</sup> The index of floods in neighboring cells is the sum of floods in cells with a common edge or vertex (queen type).

$$\Delta ntl_{it+m} = \beta_1 f_{it} + \alpha_1 wn_{it} + \nu_1 nfl_{it} + \gamma_i + \delta_t + \pi_c time_t + \omega_{pt}(month_t \times province_i) + \varepsilon_{it+m} \quad (3)$$

where I run a series of  $m$  regressions where the coefficient  $\beta_1$  of the flood indicator  $f_{it}$  associated with regression  $m$  gives the effect of a flash flood on  $\Delta ntl_{it+m}$ , the cumulative growth in nightlights between  $t - 12$  and  $t + m$ . Choosing growth relative to  $t - 12$  instead of  $t - 1$  expresses growth relative to one year ago and allows for regressions at  $t - 1$ ,  $t - 2$ , and  $t - 3$ , which is indicative of the no anticipation assumption. Variables  $wn_{it}$  and  $nfl_{it}$  are the TC damage index and the neighboring cell flood index, respectively.  $\alpha_1$  gives us the effect of a 1% increase in economic damages due to TC winds and  $\nu_1$  the local effect for a flood event in a neighboring cell.  $\gamma_i$  are cell fixed effects,  $\delta_t$  time fixed effects,  $\pi_c$  are the country  $c$  specific linear time trends, and  $\omega_{pt}$  the month of the year by province  $p$  fixed effect.<sup>9</sup> This specification removes location and time-specific averages and allows for country-specific time trends and province-specific seasonality of night light growth, reducing the remaining variation to estimate the coefficients of interest and allowing for a causal interpretation.

The dependent night light variable requires some further discussion and modeling choices. Monthly emissions at night are the average of all daily measurements without cloud coverage. For approximately 6.3% of NASA's Black Marble data in the study period, there is no cloud-free night in a month. Due to the much higher resolution of the night light compared to the rainfall data (0.25 to 6 arc-minutes or a 1 to 576 ratio of cells), the  $0.1^\circ \times 0.1^\circ$  aggregates always provide a measure of night light emission but to a varying degree of accuracy due to cloud coverage. To account for that, I linearly down-weight the panel data observations by the inverse of their share of cloud-covered Black Marble night light cells.

So far, little attention has been given to the error term. Neighboring cells likely affect the error term of the focal cell. With the current assumptions, such dependence is ruled out and potentially biases the estimation. Also, given the panel structure of the data, there is likely autocorrelation in the error term. To account for both, I use Driscoll and Kraay (1998) standard errors with an autocorrelation length of three months.

## 5 Results

Figure 4 shows impulse response functions from the model in Eq. 3 for a flash flood and a tropical storm. For both, leads up to  $t - 5$  indicate no anticipation of night lights to the hazard. A flash flood causes night light emissions to fall by around five percentage points over the course of the first five months after the incident. Then, they recover over the following months such that their impact becomes insignificant. For tropical storms, the negative effect is immediate. For each 1 percentage point increase in the hurricane damage index, night light emissions fall by around 0.8% upon impact from which they also recover in the following months.

<sup>9</sup> The province is the level one administrative sub-unit for all countries but small island states, where the province is considered equal to the country. This yields a total of 282 provinces. Examples where the country equals the province include Saint Lucia and Martinique.

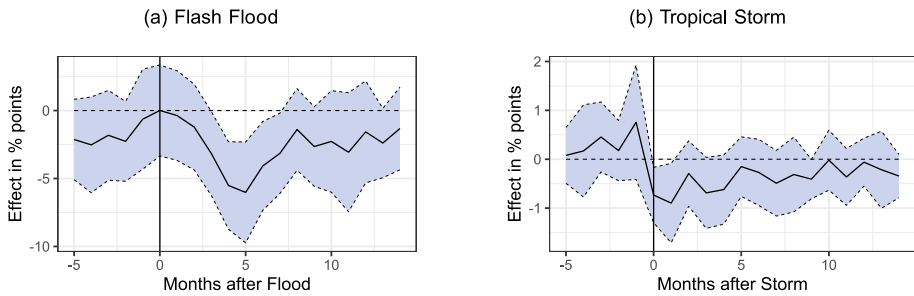


**Fig. 4** Local projection impulse response function for flash floods and tropical storms. *Notes:* Impulse response function of flash floods and tropical storms on night lights in percentage points. The black line plots the log-transformed coefficients with two-sided 95% confidence bands in blue. The regression model is as in Eq. 3 with  $\Delta ntl_{it+m}$  as the dependent variable

## 5.1 Binary Versus Continuous Measurement

Section 2.2.2 discusses the difficulty in adequately measuring flash floods via a binary indicator. To reduce the number of false positives, an IDF threshold exceedance in intensity of 2 mm/h is required in the definition of the indicator. An alternative to this informed but arbitrary cut-off is to use the threshold excess above the threshold instead of the binary indicator as a variable of interest. This reduces the weight of events barely over the threshold, which are also more likely to be false positives.<sup>10</sup> Changing the variable of interest in that manner comes at the cost of changing the interpretation of the findings to a less intuitive continuous variable. Figure 5 shows impulse response functions from the model in Eq. 3 where a threshold excess  $ex_{it}$  in mm/h is used instead of the binary indicator  $fl_{it}$ . Since the average excess is 3.9 mm/h, the estimated effect per 1 mm/h excess is smaller than in the binary case (−1.5% compared to −5%). The negative effect of a flash flood, as modeled by threshold excess, peaks again five months after the event. The IRF of the hurricane destruction index is not affected.

## 5.2 Measurement Error

Another issue with the flash flood indicator, which only approximates the true incidence of a flash flood, is that it introduces measurement error in the form of false positives and false negatives. Because the indicator is a dummy variable, the measurement error is negatively correlated with the true variable, which results in what is referred to as non-classical measurement error.<sup>11</sup> Non-classical measurement error in the exogenous variable of interest is known to bias coefficient estimates (Pischke 2007).<sup>12</sup> Modeling the flash flood incidence as continuous threshold excess likely reduces the severity of the measurement error but does not resolve it. The standard way of treatment is either by imposing additional assumptions to identify the parameters governing the bias or by using an instrumental variable

<sup>10</sup> This is assuming that the likelihood of a flash flood increases with the extremeness in rainfall.

<sup>11</sup> The continuous  $ex_{it}$  also suffers from non-classical measurement error since it still has a binary cut-off on one side.

<sup>12</sup> Interestingly, one of the earliest treatments of this issue in Aigner et al. (1973) was inspired by another paper that examines the socio-economic of a disease on the Caribbean island of St. Lucia.

(Hsiao 2022). In the case of panel data, it has been shown that the data structure can be used for an instrumental variable approach without exogenous data and relatively mild assumptions (Griliches and Hausman 1986). Specifically, assuming that the measurement error is independently and identically distributed across units  $i$  and time  $t$  and the variable with measurement error  $x_t$  is serially correlated, then one can use  $x_{t-1}$  as an instrument as long as  $T > 3$  (Hsiao 2022). In the case of the flash flood indicator, it is unlikely that there is any deviation from the iid assumption across time, while Sect. 3 indicates that there is no deviation concerning geography. In addition, the linear correlation coefficients  $Cov(fl_{it}, fl_{it-1}) = 0.1726$  and  $Cov(ex_{it}, ex_{it-1}) = 0.2236$  are statistically significantly different from zero.<sup>13</sup>

Figure 6 shows impulse response functions for flash flood rainfall excess and tropical storms where the flash flood excess  $ex_{it}$  is instrumented by  $ex_{it-1}$ . In both cases, there is no evidence for anticipation in the periods before the hazard strikes. In the flash flood excess IRF, uncertainty increases compared to the case without IV in Fig. 5, but the general size and dynamic of the effect remain the same. The IRF of tropical storms remains unchanged, with an immediate negative effect short of  $-1\%$  that recovers in the following months, as expected.

To put these results into perspective, it is of interest to consider the correlation between the three variables of interest. The correlation between  $ex_{it}$  and  $wn_{it}$  is positive but very small:  $cor(ex_{it}, wn_{it}) = 0.004$ .<sup>14</sup> This small correlation is partly driven by the much lower number of tropical storms compared to flash floods. The correlation between  $ex_{it}$  and  $exn_{it}$  is also positive and quite substantial:  $cor(fl_{it}, wn_{it}) = 0.54$ . This is owed to the much closer meteorological connection between the two variables.

### 5.3 Heterogeneity by Development

Evidence shows that flood events mainly affect low- and medium-developed countries (Loayza et al. 2012). The general development of a country could make households and firms more resilient directly or, similarly, be related to better insurance and government management of disasters. The human development index (HDI) is a summary measure of average achievement in key dimensions of human development and classifies countries into low, medium, high, and very high development.<sup>15</sup> The HDI is calculated on the country level and available for virtually all states worldwide. Some Caribbean islands are overseas territories of larger countries, such as the USA (Virgin Islands, Puerto Rico), France (Guadeloupe, Martinique), or the Netherlands (ABC Islands), for which the HDI predominantly represents mainland development. Nevertheless, these Islands boast comparatively high development and are expected to be similarly impacted by a flash flood as other very high-development states in the region, such as the Bahamas or Panama.

<sup>13</sup> Pearson's product-moment correlation suggests a 95% confidence interval of  $Cov(fl_{it}, fl_{it-1}) \in \{0.171, 0.174\}$  and  $Cov(ex_{it}, ex_{it-1}) \in \{0.222, 0.225\}$ .

<sup>14</sup> Due to the large sample size, the correlation is nonetheless statistically significant. The 95% confidence interval is  $\{0.0026, 0.0055\}$ .

<sup>15</sup> The HDI itself is often the subject of critique. For instance, it does not consider inequality directly. Still, it is a measure that, compared to GDP, is more resourceful in comparing development.

Regressing an interaction between the HDI category as of 2021 and instrumented flash flood excess rainfall onto night light growth models potential heterogeneity in effect by country development<sup>16</sup>:

$$\begin{aligned} \Delta ntl_{it+m} = & \beta(ex_{it} \times HDI_{low,high}) + \alpha(wn_{it} \times HDI_{low,high}) \\ & + v(exnfl_{it} \times HDI_{low,high}) + \gamma_i + \delta_t + \pi_c time_t \\ & + \omega_{pt}(month_t \times province_i) + \varepsilon_{it+m}. \end{aligned} \quad (4)$$

The HDI variable  $HDI_{low,high}$  is an indicator for countries with at least high development, including very high HDI and territories of European countries or the USA, and countries with low or medium HDI.<sup>17</sup> This splits the study region approximately in half, with 56% of the area falling into the low and medium HDI category, 44% into falls into the high and very high HDI category. Figure 7 shows impulse response functions from the model in Eq. 4 for flash flood excess rainfall, a tropical storm, and a flash flood in a neighboring location. IRFs are, through the interaction terms, different for low and medium HDI and high and very high HDI. Comparing the resulting IRFs, we notice that (1) low and middle HDI countries drive the negative effect of flash floods, (2) the contemporary negative effect of tropical storms is driven by high and very high HDI countries, and (3) that there is a statistically significant positive spillover effect of a neighboring flood in low and middle HDI countries. In the case of a flash flood threshold exceedance, there is no statistically significant effect for high and very high HDI countries, for both the directly effect locations as well as neighboring spillovers. In the case of tropical storms, the highly uncertain IRF for low and medium HDI countries is peculiar. A possible explanation is that, for the study period, a much smaller number of tropical cyclones hit low and medium-development countries such that the estimate is driven by two outlier hurricanes: Hurricane Matthew hitting Haiti in 2016 and Hurricane Iota hitting Nicaragua in 2020. For high and very high HDI countries, the cumulative hurricane damage index is more than 4× larger and counts around 5× more distinct storms such that any estimate is more precise and reliable. Still, a thorough investigation would be necessary to explain the origin of the tropical storms' peculiar IRF in low and medium HDI countries.

## 5.4 Heterogeneity by Geography

The economic impact of a flash flood likely depends on local characteristics. These can include the share of built-up area, terrain ruggedness, or agricultural activity. In a steeper, more rugged topography, flood currents accumulate more force and a higher share of built-up and urban area reduces the soil absorption capacity, potentially causing more detrimental impacts in case of a flood. Heterogeneity in effect by geography can be modeled via interaction, similarly to Eq. 4 with the HDI. I run separate regressions for heterogeneity in topography and heterogeneity in land use, respectively. For topography, I define four categories: flat

<sup>16</sup>  $(ex_{it} \times HDI_{low,high})$  is instrumented by  $(ex_{it-1} \times HDI_{low,high})$ . The neighboring floods are now also measured in terms of flash flood threshold excess in any neighboring locations, namely the sum of exceedances in neighboring locations  $exnfl_{it}$ , instead of being based on the binary indicator as before.

<sup>17</sup> The only country with a low HDI is Haiti. Thus, I group it with countries with a medium HDI: Guatemala, El Salvador, Honduras, Nicaragua, and Venezuela.



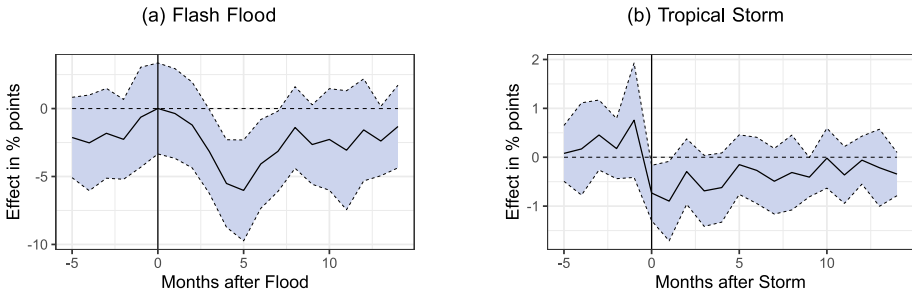


**Fig. 5** Local projection impulse response function for flash flood indicator excess intensity and tropical storms. *Notes:* Impulse response function of flash floods and tropical storms on night lights in percentage points. The black line plots the log-transformed coefficients with two-sided 95% confidence bands in blue. The flash flood impulse is excess intensity in mm/h on the binary flash flood indicator, and the tropical storm impulse is the tropical storm damage index. The regression model is as in Eq. 3 but with flash flood indicator intensity excess  $ex_{it}$  in mm/h instead of the indicator  $fl_{it}$  as the variable of interest

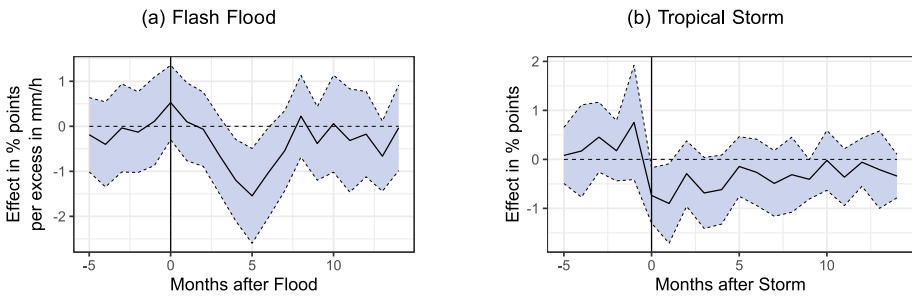


**Fig. 6** IV local projection impulse response function for flash floods and tropical storms. *Notes:* Impulse response function of flash floods and tropical storms on night lights in percentage points. The black line plots the log-transformed coefficients with two-sided 95% confidence bands in blue. The flash flood impulse is the binary flash flood indicator, and the tropical storm impulse is the tropical storm damage index. The regression model is as in Eq. 3 but with  $ex_{it}$  that is instrumented with  $ex_{it-1}$  to deal with non-classical measurement error in  $ex_{it}$  under the assumption that the measurement error is iid across time and space but  $ex_{it}$  is serially correlated

low elevation, rugged low elevation, flat high elevation, and rugged high elevation. A location is low elevation if the average elevation is below 200 m above sea level, corresponding to the 0.61% quantile. A location is rugged if the terrain ruggedness index is above 10%, corresponding to the 56% quantile. The new discrete variable  $Topography_i$  takes the four values {low and flat, low and rugged, high and flat, high and rugged} and is interacted with  $ex_{it}$ .<sup>18</sup>

$$\Delta ntl_{it+m} = \beta(ex_{it} \times Topography_i) + \alpha_1 wn_{it} + v_1 exnfl_{it} + \gamma_i + \delta_t + \pi_c time_t + \omega_{pt}(month_t \times province_i) + \epsilon_{it+m}. \tag{5}$$

Full IRF curves for different topographies from the model in Eq. 5, for both the full sample and low and medium HDI countries only, are displayed in Fig. 9 in “Appendix”. It shows

<sup>18</sup>  $(ex_{it} \times Topography_i)$  is instrumented by  $(ex_{it-1} \times Topography_i)$ .

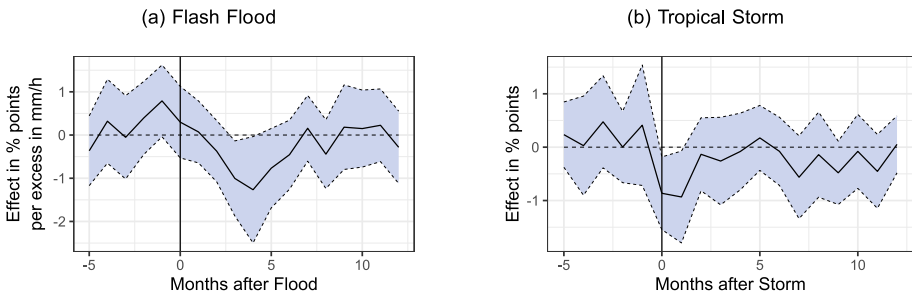


**Fig. 7** Local projection impulse response function by human development index (HDI) for flash flood indicator excess intensity, tropical storms and neighboring floods. *Notes:* Impulse response function of flash floods and tropical storms on night lights in percentage points. The black line plots the log-transformed coefficients with two-sided 95% confidence bands in blue. The regression model is as in Eq. 4. The flash flood excess intensity  $ex_{it}$  in mm/h, interacted with  $HDI_{low,high}$ , is instrumented with  $(ex_{it-1} \times HDI_{low,high})$

that the stronger impact of flash floods in low and medium development countries compared to the full sample persists when considering heterogeneity by topography. The general shape of the IDF curve is remarkably consistent as well, with a gradual increase of the negative effect reaching a maximum of four months post-flood that then recovers within the next months. Differences across topography are overall minimal and not significant. The case of rugged high elevation locations is a slight exception as they appear to be somewhat more negatively affected. Generally, topography does not matter.

For land use, I define three categories for locations dominated by built land (urban), by agriculture, or by natural land. A location is urban if 10% of the area is built, corresponding to the 0.98% quantile. A location is agriculturally dominated if the share of grassland plus cropland is above 50%, corresponding to the 66% quantile. All other locations are considered to have predominantly natural land use, including forests, shrubs, or wetlands. The new discrete variable  $Land_{urb,agr,nat}$  can be interacted with  $ex_{it}$ ,<sup>19</sup>

$$\begin{aligned} \Delta ntl_{it+m} = & \beta(ex_{it} \times Land_{urb,agr,nat}) + \alpha_1 wn_{it} + v_1 exnfl_{it} \\ & + \gamma_i + \delta_t + \pi_c time_t + \omega_{pt}(month_t \times province_i) + \varepsilon_{it+m}. \end{aligned} \tag{6}$$

Full IRF curves for different land uses from the model in Eq. 6, for both the full sample and low and medium HDI countries only, are displayed in Fig. 8 in “Appendix”. It is evident that the stronger impact of flash floods in low and medium development countries compared to the full sample persists when considering heterogeneity by land use. The general shape of the IDF curve is remarkably consistent as well, with a gradual increase of the negative effect reaching a maximum of four months post-flood that then recovers within the next months. Differences across land use are minimal and not significant.

<sup>19</sup>  $(ex_{it} \times Land_{urb,agr,nat})$  is instrumented by  $(ex_{it-1} \times Land_{urb,agr,nat})$ .

## 6 Discussion

The analysis has five main findings. First, episodes of extreme rainfall that likely trigger flash flooding have a sizeable negative effect on economic activity as measured by night light emissions. Second, the dynamics after the flood differ from a tropical storm, the arguably closest natural disaster commonly analyzed in economics. In the case of a flood, there is a slow onset of negative growth up to about months four and five before recovering in month ten. A tropical storm, in contrast, has a negative effect upon impact from where recovery is comparatively slower. This indicates that the two hazards' destruction and influence on economic activity differ. The third main finding is that a country's development influences the average impact of flash floods. A flash flood's estimated negative effect is driven by locations in low- and medium-developed countries. In addition, hurricane winds appear to have little effect on night lights in low and medium developed countries. Because the number of hurricanes in these countries was low during the study period and mainly driven by two outlier hurricanes, this tentative result should not be generalized and should be understood cautiously.<sup>20</sup> Fourth, flash floods in neighboring locations have been explored. For low and medium developed countries, a positive spillover of flash floods in terms of night light growth can be found. While the positive spillover is around 2.5× smaller than the negative direct effect of a flash flood, it indicates the existence of regional economic interactions across locations that are affected by an event. However, the spillover effects are not statistically significant for the full sample. The last main finding is that geography, if aggregated into a larger unit of analysis, does not influence flash flood risk or flash flood impact within the region of Central America and the Caribbean. Neither for refining the extreme rainfall based indicator of flash floods nor for heterogeneity in effect did elevation, terrain ruggedness, or land use matter. However, geography might well be an indispensable component for analyzing the economic impact of flash floods in another setting without spatial aggregation or by having a more climatically diverse study region (all of the study region is within the tropical climate zone).

To put the impacts of flash floods into perspective, we can compare the results with other studies on natural hazards such as hurricanes and urban floods. In the model with the excess flash flood threshold measure and IV for the whole study region, the effect of a flash flood peaks at 1.6% per mm/h in excess rainfall four months after the event. Since the average excess is 1.85, the average peak effect is a reduction in night light emissions of around 3%. The average storm reaches a damage index of 8.2 on average, which causes a reduction in night light of 6.1% and 7.4% in the month of the storm and the following month, respectively. It follows that in this study, the average flash flood event is 2× to 2.5× weaker than the average tropical cyclone in terms of night light reductions. Ishizawa et al. (2019) investigate the impacts of hurricanes on monthly economic activity in a similar setup as this study via night lights for the Dominican Republic. Their estimated effect is highly dependent on storm intensity but is said to peak 9 months after impact and go to zero after 15 months. For the average storm, the effect peaks at about -7.5%, which is again 2.5× the effect of the average flash flood as estimated in this study. Kocornik-Mina et al. (2020) study floods in the context of cities and displacement due to flood risk. They

<sup>20</sup> In terms of research on the economic impacts of hurricanes, other studies that use longer study periods are, by design, more robust. However, the finding here substantiates the question of how a country's development influences hurricane risk.

find that large floods “... reduce a city’s economic activity, as measured by nighttime lights, by between 2 and 8 percent in the year of the flood”. Since they estimate the effect in terms of yearly night light changes, their reduction between 2 and 8 percent is significantly larger than the average yearly effect found here. Equivalently averaging the point estimates of the 12 months post-flood in the model with the excess flash flood threshold measure and IV, I find an average reduction of only 0.75% for the average event. Conceptually, their focus on large-scale urban floods should lead to more substantial impacts than the narrow notion of flash floods used here: flash floods constructed via the IDF-curve approach likely generate more small-scale events than the subset of floods with at least 100,000 people displaced and detailed inundation maps in the DFO data as in Kocornik-Mina et al. (2020).

Besides the effect size, we can also distinguish between the dynamics after a flash flood (delayed negative effect) and a tropical storm (immediate negative effect). To reconcile this difference, we need to consider the type of destruction each hazard brings. Strong winds from hurricanes directly destroy buildings and damage overland power lines.<sup>21</sup> This destruction is immediately reflected in a lower night light emission and contrasts with the destruction brought by flash floods. While also destroying buildings, flash floods directly damage roads and other transportation structures which are only indirectly affected by hurricane winds (Diakakis 2020). Since most roads are unlit in Central America and the Caribbean, their destruction or deterioration does not directly cause night light emissions to fall. However, they hamper economic activity by increasing the cost of transporting goods and commuting to work (Hallegatte et al. 2016). While there is little immediate impact on night light emissions in the short term, damaged roads hinder economic activity until, after some time, repair and reconstruction are completed. This could explain the results of flash floods’ lagged effect on night lights and that more developed countries with a higher quality infrastructure are less affected. However, a better understanding of how gaps in the transportation network in developing countries affect economic activity is necessary to substantiate this explanation. For one, work has to be done to understand how firms are affected when there is a flood in their vicinity. A fruitful route might be to consider specific industries, such as construction or manufacturing, separately.

The main strength of the paper, the construction of a flash flood indicator based on physical characteristics, is also its main weakness. On one side, it allows to flexibly and consistently define a hazard across multiple countries. This is the first study in economics to rigorously define localized flood events from rainfall data directly. Others, such as Cavallo et al. (2013) and Kocornik-Mina et al. (2020), rely on event databases that are not necessarily consistent across time or countries. At the same time, by not directly observing the hazardous event but rather inferring it from a decision rule related to rainfall characteristics, I can not be certain to cover all events adequately. Strictly speaking, the results must be understood in terms of a rainfall event that likely causes some flooding in the area. Since the classification method has been calibrated on high-quality, exhaustive data for all flood events in Jamaica since 2000, it should perform well for the study region. However, extending the methodology to other regions or doing a global analysis requires appropriate calibration in each region (Hirpa et al. 2018).

Through empirical studies focusing on a specific type of natural hazard’s economic impact, we obtain a clearer picture of extreme weather’s and, in turn, climate change’s

<sup>21</sup> See the Saffir–Simpson Hurricane Wind Scale, which directly describes the damage to houses and the electricity infrastructure in its classification.

influence on the economy. The flash floods investigated here are characterized by their frequency, local occurrence, and the lagged dynamic reaction with a quick recovery. Other hazards do have different signatures on economic activity. With hurricanes, it has been suggested that their imprint on the economy is significant even several years afterward (Hsiang 2014), while droughts trigger specific migratory reactions (Kaczan and Orgill-Meyer 2020). These findings could be assessed more formally and more thoroughly in a general equilibrium growth model that considers different natural disasters and their potential trajectories concerning climate change. There is a great need for such an undertaking: most integrated assessment models assume climate change impacts to be a single, non-linear scalar of all outputs in all sectors in all locations. This omits practically all insights gained in the economic natural disasters literature. In conjunction with this neglect, it has to be noted that the uncertainty for climate change projections from economic growth is magnitudes larger than the uncertainty from the natural sciences. Thus, it is paramount for economists in the field to find precise, causal estimates for various channels through which climate change will impact the economy, natural disasters being one of them.

## 7 Conclusion

I study the dynamic effect of extreme rainfall events that lead to flash floods on local economic activity measured by night light emission in Central America and the Caribbean. The average such event decreases local emissions by up to  $-5.6\%$  in low and medium-development countries, while there is little effect in higher-development countries. The results further suggest that floods cause a different dynamic reaction to hurricanes and other natural hazards. While tropical storms reduce night light emissions upon impact, flash floods have a delayed effect that gradually accrues over the following months before recovering. In the 12 months following a flash flood, the average effect of a flood in Central America and the Caribbean is only  $-0.75\%$ , considerably lower than the effect of tropical storms or large-scale urban floods.

These findings have two main implications for policy. First, extreme rainfall episodes have a distinctly negative effect on economic activity in low and medium-developed countries. Before, the effect of extreme rainfall has often been masked by spatial or temporal aggregation. Since there appears to be little effect for higher-development countries, development in key areas could be a way out. Future research has to be conducted to investigate what those key areas are and how one can induce resilience in lower-development countries. Second, because flash floods are such a high-frequency natural hazard with return periods of less than one year in many parts of the study region, they can have direct effects on a country's economic development. In a warming and humid climate, extreme rainfall events are projected to increase in frequency and severity. I show that such an increase will likely impact the growth of developing countries in Central America and the Caribbean. Consequentially, the cost of future emissions should take this into account.

## Appendix

### Wind Field Model

The model estimates the location-specific wind speed by taking into account the maximum sustained wind velocity anywhere in the storm, the forward path of the storm, the transition speed of the storm, the radius of maximum winds, and the radial distance to the storm's eye. The model further adjusts for gust factor, surface friction, asymmetry due to the storm's forward motion, and the shape of the wind profile curve. The source of storm data used is the HURDAT Best Track Data (Landsea and Franklin 2013). These 6-hourly track data are linearly interpolated to hourly observations.  $WIND_{cst}$ , the wind experienced at any point  $i$ , during storm  $j$  at time  $t$  is given by:

$$V_{ijt} = GD \left[ V_{mjt} - S(1 - \sin(T_{ijt})) \frac{V_{hjt}}{2} \right] \times \left[ \left( \frac{R_{mjt}}{R_{ijt}} \right)^{B_{jt}} \exp \left\{ 1 - \left[ \frac{R_{mjt}}{R_{ijt}} \right]^{B_{jt}} \right\} \right]^{1/2} \quad (7)$$

where  $V_{mst}$  is the maximum sustained wind velocity anywhere in the storm,  $T_{ijt}$  is the clockwise angle between the forward path of the storm and a radial line from the storm center to the  $i$ th cell of interest,  $V_{hjt}$  is the forward velocity of the TC,  $R_{mjt}$  is the radius of maximum winds, and  $R_{ijt}$  is the radial distance from the center of the storm to point  $i$ . The remaining ingredients in Eq. (7) consist of the gust factor  $G$  and the scaling parameters  $D$  for surface friction,  $S$  for the asymmetry due to the forward motion of the storm, and  $B$ , for the shape of the wind profile curve.

In terms of implementing Eq. 7 one should note that the maximum sustained wind velocity anywhere in the storm  $V_{mst}$  is given by the storm track data, the forward velocity of the storm  $V_{hst}$  can be directly calculated by following the storm's movements between successive locations along its track, the radial distance  $R_{cst}$  and the clockwise angle  $T_{cst}$  which are calculated relative to the point of interest  $c$ . All other parameters have to be estimated or values assumed. For instance, we have no information on the gust wind factor  $G$ , but a number of studies (see e.g. Paulsen and Schroeder 2005) have measured  $G$  to be around 1.5, and I also use this value. For  $S$ , I follow Boose et al. (2004) and assume it to be 1. While we also do not know the surface friction to determine  $D$  directly, Vickery et al. (2009) note that in open water, the reduction factor is about 0.7 and reduces by 14% on the coast and 28% further 50 km inland. I thus adopt a reduction factor that decreases linearly within this range as we consider points  $c$  further inland from the coast. Finally, to determine the shape of the wind profile curve  $B$ , I employ the approximation method of Holland (1980) where  $B$  is negatively correlated with central pressure and falls in the range of 1.5–2.5 (Xiao et al. 2011). I use the parametric non-basin-specific model estimated by Vickery and Wadhera (2008) to calculate the radius of maximum winds  $R_{mst}$ .

## Land Cover

Data on the land cover are from the Copernicus Global Land Cover Layers - Collection 2 (Buchhorn et al. 2020). They provide global maps at a resolution of  $100\text{ m} \times 100\text{ m}$  for 23 land cover classes (discrete classification) or alternative ten base classes for fractional classification. Classification accuracy is 80% for the discrete case. The base classes include built-up, permanent water, tree, and cropland cover, which is sufficiently detailed for this analysis. Consolidated maps are available for the years 2015–2018. The map from 2018 is used for all the analysis as the most recent consolidate.<sup>22</sup> I use the fractional classification on the highest resolution before aggregating the fractions to the panel data cell level. That way, the fractional interpretation conserves its meaning.

## Topography

Data on topography are from Amatulli et al. (2018). They provide a suite of global topographic variables at 1 km to 100 km resolution, namely elevation and terrain ruggedness. The terrain ruggedness index (TRI) is the mean of the absolute differences in elevation between a focal cell and its 8 surrounding cells. Elevation and TRI were gathered on the highest resolution of  $1\text{ km} \times 1\text{ km}$ , and then the average for each GPM/IMERG rainfall cell was calculated.

## Heterogeneity IRFs

See Figs. 8 and 9.

---

<sup>22</sup> Arguably, land cover and flash flood severity are simultaneously and dynamically influencing each other, to some degree. Since no data is available for the whole study period, especially not on a monthly scale, the land cover data is static compared to rainfall or night light data. Note that the land cover data is only used for an exercise concerning heterogeneous effects for which the static picture of 2018 is likely a close enough approximation.

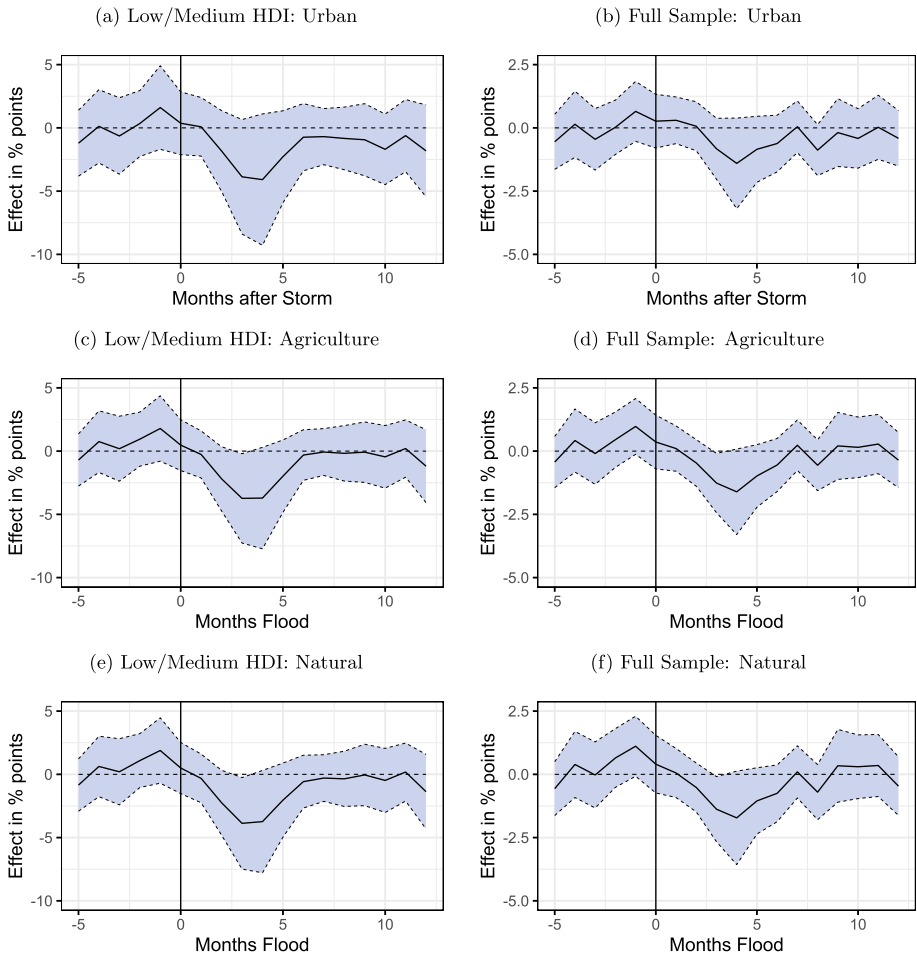
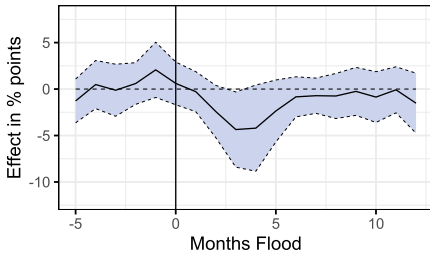


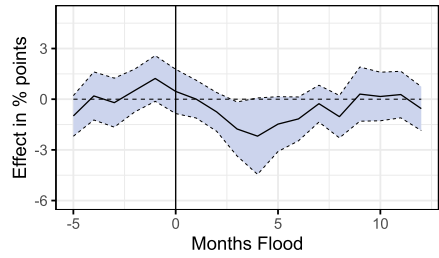
**Fig. 8** Local Projection impulse response function by dominant landuse for flash flood indicator excess intensity: full sample and low and medium HDI only. *Notes:* Impulse response function of flash floods in percentage points. The black line plots the log-transformed coefficients with two-sided 95% confidence bands in blue. The flash flood impulse is excess intensity  $ex_{it}$  in mm/h, interacted with  $Land_{urb,agr,nat}$ , and instrumented with  $(ex_{it-1} \times Land_{urb,agr,nat})$ . The regression model is as in Eq. 6



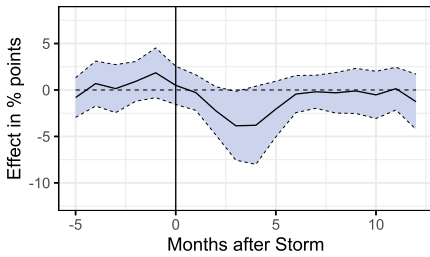
(a) Low/Medium HDI: Flat High Elevation



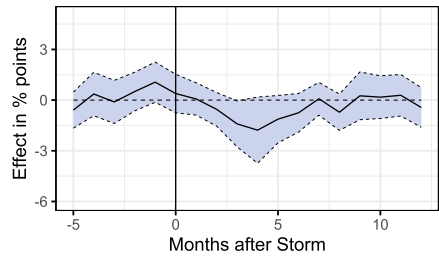
(b) Full Sample: Flat High Elevation



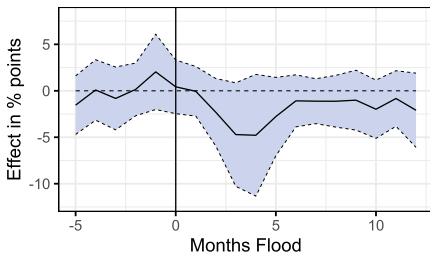
(c) Low/Medium HDI: Flat Low Elevation



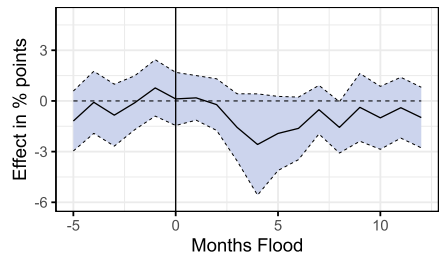
(d) Full Sample: Flat Low Elevation



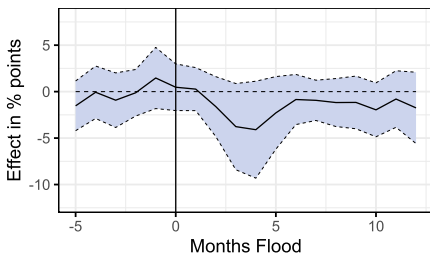
(e) Low/Medium HDI: Rugged High Elevation



(f) Full Sample: Rugged High Elevation



(g) Low/Medium HDI: Rugged Low Elevation



(h) Full Sample: Rugged Low Elevation

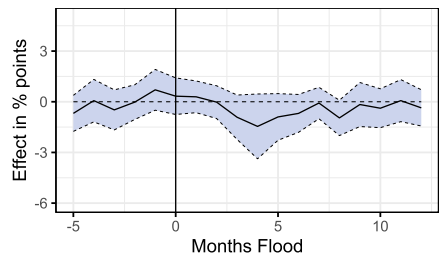


**Fig. 9** Local projection impulse response function by dominant topography for flash flood indicator excess intensity: full sample and low and medium HDI only. *Notes:* Impulse response function of flash floods in percentage points. The black line plots the log-transformed coefficients with two-sided 95% confidence bands in blue. The flash flood impulse is excess intensity  $ex_{it}$  in mm/h, interacted with  $Topography_i$ , and instrumented with  $(ex_{it-1} \times Topography_i)$ . The regression model is as in Eq. 5

**Acknowledgements** I thank two anonymous referees for helpful comments that significantly improved the paper. I am very grateful to Eric Strobl and Jeanne Tschopp for their invaluable feedback and guidance. Further thanks go to participants of the 27th Annual Conference of the European Association of Environmental and Resource Economists (2022), the Brown Bag Seminar of the University of Bern Department of Economics (2022), the Econometric Models of Climate Change Conference (2022), the Swiss Climate Summer School on Extreme Weather and Climate (2022) and the West Indies WECOM Conference (2023) for their useful comments.

**Funding** Open access funding provided by University of Bern

**Availability of data and materials** The primary data used or analyzed in this study are freely available at the indicated source. Data that result from the application of the methodology in this work are available from the corresponding author upon request.

## Declarations

**Conflict of interest** The author declares no conflict of interest. No funding was received for conducting this study.

**Open Access** This article is licensed under a Creative Commons Attribution 4.0 International License, which permits use, sharing, adaptation, distribution and reproduction in any medium or format, as long as you give appropriate credit to the original author(s) and the source, provide a link to the Creative Commons licence, and indicate if changes were made. The images or other third party material in this article are included in the article's Creative Commons licence, unless indicated otherwise in a credit line to the material. If material is not included in the article's Creative Commons licence and your intended use is not permitted by statutory regulation or exceeds the permitted use, you will need to obtain permission directly from the copyright holder. To view a copy of this licence, visit <http://creativecommons.org/licenses/by/4.0/>.

## References

- Abdelkareem M (2017) Targeting flash flood potential areas using remotely sensed data and GIS techniques. *Nat Hazards* 85(1):19–37
- Aigner DJ et al (1973) Regression with a binary independent variable subject to errors of observation. *J Econom* 1(1):49–59
- Amatulli G, Domisch S, Tuanmu M-N, Parmentier B, Ranipeta A, Malczyk J, Jetz W (2018) A suite of global, cross-scale topographic variables for environmental and biodiversity modeling. *Sci data* 5(1):1–15
- Barone G, Mocetti S (2014) Natural disasters, growth and institutions: a tale of two earthquakes. *J Urban Econ* 84:52–66
- Barrios S, Bertinelli L, Strobl E (2010) Trends in rainfall and economic growth in Africa: a neglected cause of the African growth tragedy. *Rev Econ Stat* 92(2):350–366
- Boose E, Serrano M, Foster D (2004) Landscape and regional impacts of hurricanes in Puerto Rico. *Ecol Monogr* 74:335–352
- Botzen W, Deschenes O, Sanders M (2019) The economic impacts of natural disasters: a review of models and empirical studies. *Review of Environmental Economics and Policy*
- Brei M, Mohan P, Strobl E (2019) The impact of natural disasters on the banking sector: evidence from hurricane strikes in the Caribbean. *Q Rev Econ Finance* 72:232–239
- Buchhorn M, Lesiv M, Tsendbazar N-E, Herold M, Bertels L, Smets B (2020) Copernicus global land cover layers—collection 2. *Remote Sens* 12(6):1044
- Cavallo E, Galiani S, Noy I, Pantano J (2013) Catastrophic natural disasters and economic growth. *Rev Econ Stat* 95(5):1549–1561
- Chen X, Nordhaus WD (2019) VIIRS nighttime lights in the estimation of cross-sectional and time-series GDP. *Remote Sens* 11(9):1057
- Collalti D, Spencer N, Strobl E (2024) Flash flood detection via copula-based intensity-duration-frequency curves: evidence from Jamaica. *Nat Hazards Earth Syst Sci* 24(3):873–890
- Cuaresma JC, Hlouskova J, Obersteiner M (2008) Natural disasters as creative destruction? Evidence from developing countries. *Econ Inquiry* 46(2):214–226

- Dell M, Jones BF, Olken BA (2012) Temperature shocks and economic growth: evidence from the last half century. *Am Econ J Macroecon* 4(3):66–95
- Dell M, Jones BF, Olken BA (2014) What do we learn from the weather? The new climate-economy literature. *J Econ Lit* 52(3):740–798
- Deryugina T (2017) The fiscal cost of hurricanes: disaster aid versus social insurance. *Am Econ J Econ Policy* 9(3):168–198
- Diakakis M, Deligiannakis G, Antoniadis Z, Melaki M, Katsetsiadou NK, Andreadakis E, Spyrou NI, Gogou M (2020) Proposal of a flash flood impact severity scale for the classification and mapping of flash flood impacts. *J Hydrol* 590:125452
- Driscoll JC, Kraay AC (1998) Consistent covariance matrix estimation with spatially dependent panel data. *Rev Econ Stat* 80(4):549–560
- Eichenauer VZ, Fuchs A, Kunze S, Strobl E (2020) Distortions in aid allocation of United Nations flash appeals: evidence from the 2015 Nepal earthquake. *World Dev* 136:105023
- Emanuel K (2011) Global warming effects on US hurricane damage. *Weather Climate Soc* 3(4):261–268
- Encyclopedia Britannica (2022) Central America. Website. <https://www.britannica.com/place/Central-America>
- Endreny TA, Imbeah N (2009) Generating robust rainfall intensity-duration-frequency estimates with short-record satellite data. *J Hydrol* 371(1–4):182–191
- Fabian M, Lessmann C, Sofke T (2019) Natural disasters and regional development—the case of earthquakes. *Environ Dev Econ* 24(5):479–505
- Felbermayr G, Gröschl J (2014) Naturally negative: the growth effects of natural disasters. *J Dev Econ* 111:92–106
- Felbermayr G, Gröschl J, Sanders M, Schippers V, Steinwachs T (2022) The economic impact of weather anomalies. *World Dev* 151:105745
- Fomby T, Ikeda Y, Loayza NV (2013) The growth aftermath of natural disasters. *J Appl Econ* 28(3):412–434
- Gibson J, Olivia S, Boe-Gibson G, Li C (2021) Which night lights data should we use in economics, and where? *J Dev Econ* 149:102602
- Griliches Z, Hausman JA (1986) Errors in variables in panel data. *J Econom* 31(1):93–118
- Hallegatte S, Dumas P (2009) Can natural disasters have positive consequences? Investigating the role of embodied technical change. *Ecol Econ* 68(3):777–786
- Hallegatte S, Dumas P, Hourcade J-C, Dumas P (2007) Why economic dynamics matter in assessing climate change damages: illustration on extreme events. *Ecol Econ* 62(2):330–340
- Hallegatte S, Vogt-Schilb A, Bangalore M, Rozenberg J (2016) Unbreakable: building the resilience of the poor in the face of natural disasters. World Bank Publications, Washington
- Henderson JV, Storeygard A, Weil DN (2012) Measuring economic growth from outer space. *Am Econ Rev* 102(2):994–1028
- Hirpa Feyera A, Salamon P, Beck HE, Lorini V, Alfieri L, Zsoter E, Dadson SJ (2018) Calibration of the Global Flood Awareness System (GloFAS) using daily streamflow data. *J Hydrol* 566:595–606
- Hodler R, Raschky PA (2014) Economic shocks and civil conflict at the regional level. *Econ Lett* 124(3):530–533
- Holland G (1980) An analytic model of the wind and pressure profiles in hurricanes. *Mon. Weather Rev.* 106:1212–1218
- Hornbeck R (2012) The enduring impact of the American Dust Bowl: short-and long-run adjustments to environmental catastrophe. *Am. Econ. Rev.* 102(4):1477–1507
- Houknepè J, Diekkrüger B, Afouda AA, Sintondji LOC (2019) Land use change increases flood hazard: a multi-modelling approach to assess change in flood characteristics driven by socio-economic land use change scenarios. *Nat. Hazards* 98:1021–1050
- Hsiang SM, Jina AS (2014) The causal effect of environmental catastrophe on long-run economic growth: evidence from 6,700 cyclones. National Bureau of Economic Research, Technical Report
- Hsiao C (2022) Analysis of panel data number, vol 64. Cambridge University Press, Cambridge
- Huffman GJ, Bolvin DT, Nelkin EJ et al (2015) Integrated Multi-satellite Retrievals for GPM (IMERG) technical documentation. NASA/GSFC Code 612(47):2019
- IPCC (2023) Climate change 2023: synthesis report. Summary for policymakers. In: Lee H, Romero J (eds) Contribution of working groups I, II and III to the sixth assessment report of the intergovernmental panel on climate change. Core Writing Team, pp 1–34
- Ishizawa Oscar A, Miranda JJ (2019) Weathering storms: understanding the impact of natural disasters in Central America. *Environ Resour Econ* 73:181–211
- Ishizawa OA, Miranda JJ, Miranda JJ, Strobl E (2019) The impact of Hurricane strikes on short-term local economic activity: evidence from nightlight images in the Dominican Republic. *Int J Disaster Risk Sci* 10(3):362–370
- Jordà Ò (2005) Estimation and inference of impulse responses by local projections. *Am Econ Rev* 95(1):161–182

- Kaczan DJ, Orgill-Meyer J (2020) The impact of climate change on migration: a synthesis of recent empirical insights. *Clim Change* 158(3–4):281–300
- Klomp J (2016) Economic development and natural disasters: a satellite data analysis. *Glob Environ Change* 36:67–88
- Klomp J, Valckx K (2014) Natural disasters and economic growth: a meta-analysis. *Glob Environ Change* 26:183–195
- Kocornik-Mina A, McDermott TK, Michaels G, Rauch F (2020) Flooded cities. *Am Econ J Appl Econ* 12(2):35–66
- Kotz M, Levermann A, Wenz L (2022) The effect of rainfall changes on economic production. *Nature* 601(7892):223–227
- Koutsoyiannis D, Kozonis D, Manetas A (1998) A mathematical framework for studying rainfall intensity-duration-frequency relationships. *J Hydrol* 206(1–2):118–135
- Kunze S (2021) Unraveling the effects of tropical cyclones on economic sectors worldwide: direct and indirect impacts. *Environ Resour Econ* 78(4):545–569
- Landsea CW, Franklin JL (2013) Atlantic hurricane database uncertainty and presentation of a new database format. *Mon Weather Rev* 141:3576–3592
- Lazzaroni S, van Bergeijk PAG (2014) Natural disasters' impact, factors of resilience and development: a meta-analysis of the macroeconomic literature. *Ecol Econ* 107:333–346
- Loayza NV, Olaberria E, Rigolini J, Christiaensen L (2012) Natural disasters and growth: going beyond the averages. *World Dev* 40(7):1317–1336
- Naguib C, Pelli M, Poirier D, Tschopp J (2022) The impact of cyclones on local economic growth: evidence from local projections. *Econ Lett* 220:110871
- Nordhaus WD (2010) The economics of hurricanes and implications of global warming. *Clim Change Econ* 1(01):1–20
- Noy I, Strobl E (2023) Creatively destructive hurricanes: do disasters spark innovation? *Environ Resour Econ* 84(1):1–17
- Panwar V, Sen S (2020) Disaster damage records of EM-DAT and DesInventar: a systematic comparison. *Econ Disasters Clim Change* 4(2):295–317
- Paulsen B, Schroeder J (2005) An examination of tropical and extratropical gust factors and the associated wind speed histograms. *J Appl Meteorol* 44:270–280
- Pinos J, Quesada-Román A (2021) Flood risk-related research trends in Latin America and the Caribbean. *Water* 14(1):10
- Pischke S (2007) Lecture notes on measurement error. London School of Economics, London
- Román MO, Wang Z, Sun Q, Kalb V, Miller SD, Molthan A, Schultz L, Bell J, Stokes EC, Pandey B et al (2018) NASA's Black Marble nighttime lights product suite. *Remote Sens Environ* 210:113–143
- Seneviratne SI, Zhang X, Adnan M, Badi W, Dereczynski C, Di Luca A, Ghosh S, Iskander I, Kossin J, Lewis S et al (2021) Weather and climate extreme events in a changing climate (Chapter 11)
- Skidmore M, Toya H (2002) Do natural disasters promote long-run growth? *Econ Inquiry* 40(4):664–687
- Storeygard A (2016) Farther on down the road: transport costs, trade and urban growth in sub-Saharan Africa. *Rev Econ Stud* 83(3):1263–1295
- Strobl E (2011) The economic growth impact of hurricanes: evidence from US coastal counties. *Rev Econ Stat* 93(2):575–589
- Strobl E (2012) The economic growth impact of natural disasters in developing countries: evidence from hurricane strikes in the Central American and Caribbean regions. *J Dev Econ* 97(1):130–141
- Strulik H, Trimborn T (2019) Natural disasters and macroeconomic performance. *Environ Resour Econ* 72:1069–1098
- Vickery P, Masters F, Powell M, Wadhwa D (2009) Hurricane hazard modeling: the past, present, and future. *J Wind Eng Ind Aerodyn* 97:392–405
- Vickery Peter J, Dhiraj W (2008) Statistical models of Holland pressure profile parameter and radius to maximum winds of hurricanes from flight-level pressure and  $H^*$  Wind data. *J Appl Meteorol Climatol* 47(10):2497–2517
- Wheaton H, Evans E (2009) Land use, water management and future flood risk. *Land Use Policy* 26:S251–S264
- Xiao YF, Duan ZD, Xiao YQ, Ou JP, Chang L, Li QS (2011) Typhoon wind hazard analysis for southeast China coastal regions. *Struct Saf* 33(4–5):286–295